

1 **A balaenopterid from the Lower Pleistocene of southern Italy and the Quaternary**
2 **baleen whales (Cetacea, Mysticeti) of the Mediterranean**

3

4

5 Andrea Zazzera¹, Angela Girone¹, Rafael La Perna¹, Maria Marino¹, Patrizia Maiorano¹, Raffaele
6 Sardella², Vincenza Montenegro³, Ruggero Francescangeli^{1,3}, Giovanni Bianucci⁴

7 ¹ Dipartimento di Scienze della Terra e Geoambientali, Università degli Studi di Bari Aldo Moro,
8 Italy;

9 ² Dipartimento di Scienze della Terra, Università di Roma La Sapienza, Italy;

10 ³ SIMA (Sistema Museale di Ateneo), Università degli Studi di Bari Aldo Moro, Italy;

11 ⁴Dipartimento di Scienze della Terra, Università di Pisa, Italy

12 * Corresponding author: e-mail: giovanni.bianucci@unipi.it

13

14 **Abstract**

15 An almost complete and partially articulated skeleton of an Early Pleistocene baleen whale is here
16 described. The fossil, measuring 11 m in length, was discovered in the Calcarene di Gravina
17 Formation at Lama Lamasinata site (Bari, southern Italy) in 1968. The bifurcated first rib combined
18 with other characters supports the identification of the fossil whale as a possible undescribed
19 species of *Balaenoptera* (Mysticeti, Balaenopteridae), close to or nested in the *B. borealis* - *B.*
20 *edeni*- *B. ricei* clade. However, the limited number of preserved diagnostic characters suggests a
21 prudent assignation of the Bari whale to *Balaenoptera* sp. The associated molluscs suggest a mid-
22 shelf setting deposition near to the boundary between infralittoral and circalittoral environments,
23 probably 40-60 m deep. An associated *Carcharodon carcharias* tooth and shark bite marks on a rib
24 support the hypothesis that an early scavenger action prevented the rising of the whale carcass
25 because of the removal of abdominal tissues and the consequent reduction of the decomposition gas

26 accumulation. The occurrence of chemosymbiotic bivalves near the skeleton could testify the
27 development of the sulphophilic stage during decay. The Bari specimen sheds new light on the
28 diversity and disparity of the mysticete fauna in the Mediterranean Pleistocene also related to the
29 geodynamic, palaeoclimatic and palaeoceanographic conditions that favoured upwelling events and
30 nutrients supply into the southern Adriatic basin.

31

32 **Key-words:** Mysticeti, *Balaenoptera*; Pleistocene, Mediterranean, Taphonomy, Palaeoceanography

33

34 **1. Introduction**

35 For some centuries, several naturalists and palaeontologists reported significant fossil remains of
36 baleen whales (Cetacea, Mysticeti) from Neogene deposits of Italy (Bianucci, 2014; Collareta et al.
37 2020). These discoveries provided a significant dataset potentially useful to reconstruct the changes
38 in the composition and structure of the Mediterranean mysticete fauna, partially related to the
39 complex geodynamic and climatic history of this basin.

40 Italian baleen whale remains have been found beginning since the middle Miocene (e.g., Bisconti,
41 2006, 2010), to become extraordinarily frequent in the Pliocene clays and sands exposed in the hills
42 of Tuscany, Piedmont and Emilia Romagna (e.g., Bisconti, 2009; Bisconti et al. 2020). On the whole,
43 this well-known Pliocene fossil assemblage indicates that in the Mediterranean during this epoch
44 lived an highly diversified mysticete fauna represented by balaenids, basal balaenopteroids,
45 balaenopterids, cetotheriids and eschrichtiids.

46 By contrast, the Pleistocene baleen whale fauna is poorly known and only on a fragmentary fossil
47 record mostly based on rare and recent discoveries. Preliminary studies on these fossil remains (Tsai
48 et al. 2017; Bianucci et. al. 2019), together with indirect observations based on the analysis of fossil
49 whale barnacles (Collareta et al. 2016, 2018a,b), evidenced the presence of balaenids, balaenopterids,
50 and neobalaenids in the Pleistocene Mediterranean Sea. However, this scenario is still poorly defined

51 and, for example, it does not yet allow to understand the causes which led to the present dramatical
52 low diversity of baleen whales in the Mediterranean. In fact, today only one mysticete species, the fin
53 whale *Balaenoptera physalus*, regularly frequents the Mediterranean (Notarbartolo-Di-Sciara et al.,
54 2003). In particular, the few data on the Mediterranean Quaternary mysticete assemblage are not
55 sufficient to clarify if the decline in diversity started in the Pleistocene, possibly related to the Plio-
56 Pleistocene turnover observed on a global scale (Marx et al., 2016), or if it is an even more recent
57 phenomenon only affecting the Mediterranean.

58 Notwithstanding the necessity to better investigate the mysticete Pleistocene paleocommunity of the
59 Mediterranean, the scarcity of cetacean fossil record of this period is a global phenomenon that has
60 been related to the Holocene sea level rising making these fossils inaccessible beneath the ocean floor
61 (Marx et al., 2016; Bianucci et al., 2019). Recently, a taphonomic explication has also been proposed:
62 the progressive increase of the efficiency of bone-eating bioeroders reduced the preservation of whale
63 skeletons (Dominici et al., 2020).

64 Therefore, the diversity and numerical consistency of fossil mysticetes in the Pleistocene
65 Mediterranean deposits appear to be the result of a combination of factors on global and regional
66 scale, as well as of selective taphonomic processes.

67 In the present work, an almost complete skeleton of a baleen whale is described. It was discovered in
68 1968 from the Lower Pleistocene calcarenites exposed at Lama Lamasinata site (Bari, southern Italy)
69 (Fig. 1A). A new view of the Mediterranean mysticete fauna in the Quaternary is herein proposed,
70 based on systematic and taphonomic observations, and on palaeoceanographic considerations.

71

72 **2. Material and methods**

73 *2.1. Institutional abbreviations*

74 **BM**, British Museum, London, England; **GNHM**, Gamagori Natural History Museum, Japan; **MB**,
75 Museum für Naturkunde, Berlin, Germany; **MSNUP**, Museo di Storia Naturale, Università di

76 Pisa;Calci (Pisa), Italy; **MST**, Museo Scienze della Terra, Dipartimento di Scienze della Terra e
77 Geoambientali, Università degli Studi di Bari Aldo Moro, Italy; **SAM**, South Australia Museum,
78 Adelaide, Australia; **WMA**, Whale Museum, Ayukawa, Japan; **WRI**, Whales Research Institute,
79 Tokyo, Japan.

80

81 *2.2. Anatomical terminology*

82 The anatomical terminology follows Mead and Fordyce (2009) for the skull, Ekdale et al. (2011) for
83 the tympanic bulla, and Evans and de Lahunta (2012) for the postcranial skeleton.

84

85 **3. Systematic palaeontology**

86 Cetacea Brisson, 1762

87 Mysticeti Gray, 1864

88 Chaeomysticeti Mitchell, 1989

89 Balaenopteridae Gray, 1864

90 *Balaenoptera* Lacepede, 1804

91 *Balaenoptera* sp.

92 Figures 2-5, Table 1

93

94 **Referred specimen.** Partially articulated almost complete 11 m long skeleton, still partially
95 embedded in hard matrix and exposed dorsal side-up, kept at the Museo di Scienze della Terra,
96 Università degli Studi di Bari Aldo Moro with access number MSTQ1 (Fig. 2). It consists of:
97 fragmentary cranium; both mandibles; right and left tympanic bullae (the left removed by the
98 matrix); vertebral column lacking of the atlas, some thoracics and the posterior caudals; nine right
99 and nine left ribs, more or less complete; right scapula, radius, ulna, carpal?, and phalanx; left
100 radius and ulna.

101 **Preservation state.** A significant part of the dorsal portion of almost all the bones was destroyed
102 during the canal excavation. Moreover most of the bones are still partially covered by sediment and
103 for several bones only their cutting section is visible and consequently only the bidimensional shape
104 can be observed. Unfortunately, the cranium, the most diagnostic skeletal element of neocetes, was
105 seriously damaged, before burial and fossilization, and during the canal excavation.

106 **Locality, horizon and age.** This skeleton was discovered in 1968 by Enzo Indraccolo, Vittorio
107 Stagnani, Oreste Triggiani, and Nicola Cervini in an artificial drainage channel at Lama Lamasinata
108 site in the northern part of Bari town (Puglia, southern Italy) (Montenegro, 2016). The sediment
109 embedding the fossil belongs to the Gelasian?-Calabrian (Lower Pleistocene) Calcarene di Gravina
110 Formation, a carbonate unit exposed extensively in Apulia region and usually showing shoreface to
111 offshore transition facies associations (Pieri et al., 2011) (Fig. 1A). Unfortunately, a more precise age
112 was not possible, due to the poorly preserved calcareous nannofossil assemblages observed in
113 examined sediments collected for biostratigraphy near the skeleton. However, the occurrence of
114 *gephyrocapsids* > 3-4 μm allows an early Calabrian age to be inferred, at least tentatively, according
115 to Rio et al.(1990).

116 **Ontogeny.** The vertebral epiphyses are free and disarticulated from the centra in all preserved
117 thoracics posterior to T2 one and in the first and fifth lumbar posterior to the last preserved rib. In
118 the other vertebrae (all the cervicals, the first two thoracics and most of the lumbar and caudals)
119 the epiphyses are joined to their respective corpora, although sutures are always clearly visible
120 except for the last preserved caudals. This ossification pattern is compatible with that observed in 9-
121 year-old male and 13-year-old female *Balaenoptera acutorostrata* (Kato, 1988). The body size of a
122 such sexually mature, but not physically mature, whale is already close to that of an adult (Kato,
123 1988). A similar ossification pattern, with the epiphyses of the thoracic vertebrae, the last to join the
124 respective centra, is common in both mysticetes (Kato, 1988; Kemper and Leppard, 1999) and
125 odontocetes (Galatius and Kinze 2003).

126 **Total body length estimate.** The total body length (hereafter TBL) of MST Q1 was estimated 12.28

127 m using a mandible length value of 271 cm by means the Pyenson et al. (2013) equation.

128 **Remarks on the systematic assignation.** MSTQ1 belongs to a baleen-bearing mysticete
129 (Chaecomysticeti) by having edentulous laterally bowed mandibles with short unfused symphysis; it
130 belongs to a Balaenopteridae by having the mandible with a sinusoidal dorsal outline and the
131 tympanic bulla with an anterolateral shelf and with involucral and main ridges not coincident. It is
132 referred to the genus *Balaenoptera* by having double-headed first rib, a peculiar character only
133 shares with *Balaenoptera borealis* and *B. edeni*, two species well nested within the *Balaenoptera*
134 clade.

135 **Description.** Cranium. Unfortunately, the cranium is almost totally lost, being a portion of the
136 basicranium and some isolated pieces of flat rostral bones the only preserved remains (Fig. 3). The
137 well preserved flat dorsal surface of the basioccipital is exposed between the disarticulated
138 squamosals. The squamosals lacks the zygomatic processes and their dorsal surface is badly
139 preserved. On the left anterior side of the preserved portion of the neurocranium, between the
140 squamosal and the basioccipital, is visible a fragmentary bone that could be a piece of the left
141 pterygoid. Another larger and anteroposteriorly elongated bone, possibly a portion of the right
142 palatine, lies anteriorly to the basioccipital. Anteriorly to the basicranium, between the two mandibles,
143 some displaced fragments of bones are exposed. The two largest fragments consists of two flat sheets
144 referable to rostral portions of the maxilla.

145 Tympanic bulla. In dorsal view the tympanic bulla exhibits a reniform shape with its medial margin,
146 corresponding to the main ridge, regularly arcuated (Fig. 4). On the dorsal surface the involucral
147 ridge is weak but clearly distinct along the anteroposterior length of the bone. This ridge is laterally
148 retracted from the medial margin of the tympanic bulla for most of its extension but reaches the
149 main ridge at the anterior corner of the tympanic bulla. The dorsolateral surface of the involucrum
150 is sculptured by weak transverse creases and the Eustachian opening is transversally narrow. The
151 well-developed sigmoid process is positioned posterior to the transverse middle line, it is
152 perpendicular to the main axis of the bone, and its posterior margin is straight. In medial view, an

153 almost straight dorsal margin (corresponding to the involucrel surface) and a convex and half circle-
154 shaped ventral margin are well visible. The main ridge extend anteroposteriorly along the main axis
155 of the bone. The lateral surface is well exposed in the right bulla, although its posterior portion,
156 including the conical process, is partially covered by the transverse process of the second cervical.
157 The lateral furrow is deep and transversely oriented and the involucrel surface is planar. The
158 anterolateral shelf was present, although only partially preserved in the right tympanic bulla and
159 completely lost due to breakage in the left bulla. The ventral surface is covered by the sediment in
160 the right tympanic bulla and it is seriously damaged in the left bulla. The latter presents most of the
161 ventral wall missing and consequently only the mold of the internal cavity is visible in ventral view.

162 Mandible. Both mandibles are preserved in anatomical position (Fig. 3A). Although their general
163 outline is roughly traceable, they are strongly abraded and therefore some anatomical parts,
164 significant for the systematic determination are missing (e.g. coronoid process) or badly preserved
165 (e.g. mandibular condyle). In dorsal view, the mandibles are moderately bowed laterally with the
166 mandibular condyle projecting posterolaterally, with a distinct mandibular neck. Consequently the
167 entire lateral outline of the mandible is sigmoid in shape. The two mandibles converge
168 anteromedially without any contact between them, being the very short symphysis unsutured. Trace
169 of the vestigial alveolar groove is discernible near and parallel to the dorsomedial margin of the
170 mandible.

171 Cervical vertebrae. The atlas is missing whereas the C2-C7 are preserved, articulated and unfused
172 (Fig. 3B,C). Only the half ventral part of the centra and the ventral transverse processes of C2-C7 of
173 MST Q1 are preserved, even if all more or less covered by sediment. The length of the centra is almost
174 constant, ranging from 4.1 to 6.1 cm, with C3 and C4 slightly shorter than the other cervical centra
175 (Tab. 1). The broken surfaces of the vertebrae clearly show the epiphyses well sutured to the centra,
176 although the sutural surfaces are well discernible. When exposed, the dorsal surface of the ventral
177 transverse processes show some breakages, suggesting a missing proximal dorsal widening of the
178 ventral transverse processes that could have been originally joined with the dorsal transverse

179 processes forming wide vertebroarterial foramina.

180 Thoracic vertebrae. The first two thoracic vertebrae are in anatomical connection (T1 articulated with
181 the C7 and with T2), whereas the other preserved thoracics show a progressive degree of
182 disarticulation toward the posterior portion of the skeleton (Fig. 3B,C). The preserved right transverse
183 processes of T1-T3 are anterolaterally directed. The length of the centra increases progressively
184 posteriorly passing from 7.8 cm in T1 to slightly more than 10 cm in T4 and T5. The epiphyses are
185 fused to the vertebrae in T1 and T2 and more or less unfused and disarticulated in the other preserved
186 thoracics. The original number of thoracics is unknown since the posteriormost thoracics are missing
187 or badly preserved. However, the minimal possible number of thoracics is nine, as indicated by the
188 number of ribs preserved in both the right and the left side.

189 Lumbar and caudal vertebrae. About 22 articulated lumbar and caudal vertebrae, for a total length of
190 9.5 m, are exposed posteriorly to the disarticulated rib cage (Fig. 2). Nevertheless, only the
191 longitudinal sections of the centrum of these vertebrae are visible on the surface of the stone slab.
192 The sections do not necessary cross the maximum diameter of the centra and therefore they provide
193 just information about the maximum length of the centra but not about the maximum width. In
194 particular, it can be observed that the length of the centrum progressively increases towards the back,
195 and then decreases in the last six preserved centra, probably belonging to caudals. Since the ventral
196 surface of the vertebrae is not exposed, it is not possible to observe if the vertebral tubercles for
197 chevrons are present and consequently it is not possible to recognize the limit between lumbar and
198 cervicals.

199 Ribs. Nine right ribs and nine left ribs, more or less complete, are exposed on the large slab of
200 calcarenite stone (Figs 2, 3B,C). Although disarticulated, the ribs are close to their life position. The
201 first left rib, partially covered by other ribs and sediment, is double-headed, shorter than the other
202 ribs, and distally widened (Fig. 5A,B). The bifurcation affects the proximal ca 20 cm of the first rib
203 and the two headed portions have approximately the same size. The first right rib is still partially
204 articulated with the dorsal transverse process of C7 and lacks one of the heads for breakage. Only a

205 small proximal portion of the second left rib is visible, whereas the third and fourth left ribs are well
206 exposed above the first left rib. The second and the third ribs are similar in length and show the same
207 L-shape, due to an almost-right-angle formed by their proximal portion (tuberculum and capitulum)
208 with the roughly straight main body of the rib. The next preserved ribs are slender and more regularly
209 curved.

210 Forelimbs. The right scapula, exposed in medial view, is incomplete lacking its half posterior
211 portion (Fig. 5D,E). Moreover its margins are partially eroded and consequently its outline cannot
212 be reconstructed in detail. A fragment of bone placed near the head of the right humerus could be a
213 part of the missing ventral portion of the scapula. The acromion is elongated, apparently slender
214 (but it is rather eroded) and its main axis roughly forms a straight angle with the vertical axis of the
215 scapula. Only an eroded longitudinal section of the right humerus is preserved, providing the
216 silhouette of this bone. It is moderately short (length humerus/length radius: ca 0.55), moderately
217 robust (width at middle length/length: ca 0.39, but the width could be sub-estimated due to the bad
218 preservation), straight, and slightly distally widened. Its half circled head represents the 31% of the
219 total humerus length, but also for this feature it needs some caution due to the fragmentary state of
220 the bone. The radial and ulnar facets form an angle of ca 135 degrees. The radius is slender (width
221 at middle length/length: ca 0.13) and slightly curved (Fig. 5F,G). Its distal epiphysis is not well
222 preserved in both right and left radius. The left ulna bears a large olecranon process extending
223 significantly more proximal than the proximal anterior corner of the ulna (i.e. coronoid process).
224 However, it is not possible to reconstruct the exact shape of the olecranon since its distal margin is
225 broken. The ulna is even slender than the radius (width at middle length/length: ca 0.12) and more
226 arcuated (posterior margin distinctly convex). It slightly widens distally. A small globose bone in
227 contact with the distal epiphysis of the right radius could be a carpal and more specifically,
228 considering its position in respect to the radius, the scaphoid. However, its irregular shape due to
229 bad preservation and/or original partial ossification prevents a sure identification of this small bone.
230 About 20 cm from the distal epiphysis of the right radius and ulna is a phalange partially covered by

231 the fourth left rib. Its well exposed proximal articulation is concave.

232 **Comparison.** Body size. The body size estimations reported above indicate a TBL for MST Q1 of
233 about 12 m and some considerations made on the ontogenetic stage suggest that this whale died
234 when sexually mature and very close to be fully adult. Among balaenopterids, such size falls within
235 the average male-female TBLs of adults of extant *Balaenoptera omurai* (ca 10-12 m), *B. ricei* (ca
236 11-12 m), and *Megaptera novaeangliae* (ca 12-14 m). Balaenopterids with TBL larger than that
237 estimated for MST Q1 are the extant *Balaenoptera edeni* (ca 13-14 m), *B. borealis* (ca 14-15), and
238 *B. physalus* and *B. musculus*, both exceeding 20 m in length. By contrast, the extant *Balaenoptera*
239 *bonaerensis* and *B. acutorostrata*, both roughly 8-9 m in length, are smaller than MST Q1.
240 Compared with the fossil balaenopterids, the estimated TBL of MST Q1 is larger than in *Incakujira*
241 *anillodefuego* (8.2 m; Marx and Kohno, 2016) and '*Megaptera*' *hubachi* (8.5 mm; Lambert et al.
242 2010).

243 Cranium. Due to its fragmentary state, no diagnostic characters were detected in the MST Q1
244 cranium. However, if we assume that the mandibles have not significantly dislocated from their
245 original anatomical position, the bizygomatic width of the cranium may havenot been very large in
246 relation to the length of the cranium. Therefore, we could exclude the appurtenance of MST Q1 to
247 the genus *Megaptera* whose zygomatic processes of the squamosal significantly extend laterally
248 generating a wide cranium.

249 Tympanic bulla. The MST Q1 tympanic bulla exhibits a synapomorphy of the balaenopterids: the
250 presence of an anterolateral shelf (state 1 of char. 7 in Ekdale et al. 2011). This shelf is partially
251 preserved in the right bulla and missing for breakage in the left bulla.

252 The size of the MST Q1 tympanic bulla (total length: 100 mm) is close to *Balaenoptera*
253 *bonaerensis* (90-100 mm), slightly larger than *B. acutorostrata* (78-94 mm) and larger than all other
254 extant balaenopterids. In this regard it is important to underline that the tympanic bulla does not
255 grow significantly after birth in a mysticete (Cozzi et al., 2012; G.B. pers. obs.) and therefore the
256 size of the tympanic bulla of the estimated sexually mature MST Q1 whale was probably very close

257 to the size of an adult animal. Compared with the fossil balaenopterids, the length of MST Q1
258 tympanic bulla is slightly larger than in *Incakujira anillodefuego* (89.5 mm; Marx and Kohno,
259 2016) and close to *Plesiobalaenoptera quarantellii* (97-98 mm; Bisconti, 2010).

260 The MST Q1 tympanic bulla differs from *Balaenoptera musculus* by not having a dorsal posterior
261 prominence (state 1 of char. 5 in Ekdale et al., 2011), a posteriorly extended involucrum (state 1 of
262 char. 10 in Ekdale et al., 2011), a dorsal involucral surface in medial view markedly sinuous and
263 strong concave (state 1 of char. 11 in Ekdale et al., 2011), and a sigmoid process located
264 approximately at the transverse midline. The MST Q1 tympanic bulla differs from *Balaenoptera*
265 *musculus* and *B. physalus* by not having an elevated and flattened posterior portion of medial
266 margin of main ridge (state 1 of char. 13 in Ekdale et al. 2011) and a sigmoid process with a linear
267 posterior margin. The MST Q1 tympanic bulla differs from *Balaenoptera acutorostrata* and *B.*
268 *bonaerensis* by having a more robust sigmoid process and by not having a planar dorsal surface of
269 the involucrum adjacent to the Eustachian opening (state 1 of char. 12 in Ekdale et al., 2011), and an
270 involucral ridge extends further anterior than main ridge (state 1 of char. 17 in Ekdale et al., 2011).

271 The MST Q1 tympanic bulla differs from *Megaptera novaeangliae* by having an involucral ridge
272 retracted from the posterior end of the bulla (state 0 of char. 16 in Ekdale et al., 2011) and a
273 narrower eustachian opening; moreover the tympanic bulla of *M. novaeangliae* exhibits a unusual
274 inflated shape well evidenced in ventral view by the broadly rounded ventral margin. The MST Q1
275 tympanic bulla mainly differs from *Incakujira anillodefuego* for the shape of the sigmoid process,
276 straight and with a linear posterior margin in MST Q1 and slightly anteriorly deflected in *I.*
277 *anillodefuego* (Marx and Kohno, 2006). The tympanic bulla of *Plesiobalaenoptera quarantellii*
278 seems to have a more globose shape in dorsal and ventral view and the sigmoid process nearer to
279 the transverse midline (Bisconti, 2010a). The remaining balaenopterids whose tympanic bulla is well
280 known, namely the extant *Balaenoptera borealis*, *B. edeni* and *B. omurai*, have the tympanic bulla
281 compatible in shape with the one of MST Q1. Unfortunately, due to the incompleteness and the
282 partially covering by sediment, a more detailed comparison of the MST Q1 tympanic bulla with

283 these three balaenopterid species is not possible.

284 Mandible. Unfused symphysis and absence of functional alveoli observed in the MST Q1 mandible
285 are characters shared with all the baleen-bearing mysticetes (Chaecomysticeti). The sigmoid shape of
286 the MST Q1 mandible, due to the combination of a moderate curvature with a mandibular neck
287 slightly posterolaterally recurved, is a derived character of the balaenopterids.

288 Ribs. A peculiar double-headed first rib such as in MST Q1 was only observed in *Balaenoptera*
289 *borealis* (Fig. 5C) and *B. edeni* among the other cetaceans (Van Beneden and Gervais, 1869-1879,
290 pl. 15, fig. 34; Andrews, 1916, fig. 30; Omura, 1959pl. 6, fig. 1; Nishiwaki and Kasuya, 1971pl. 2,
291 fig. 6; Omura et al. 1981, fig. 7; Kinze, 2005, fig. 2; pers. obs.). This rib bifurcation clearly differs
292 from that described by Buchholtz (2011) in *Caperea marginata* and also from the anomalies
293 observed in some individuals of *Eschrichtius robustus* and *Balaenoptera musculus* (Fig. 6).
294 In *C. marginata* the first rib is two-headed in the juvenile stage but subsequently expands distally
295 changing its shape from a single medial head to a triangular bifurcated plate of variable width in the
296 adults (Buchholtz et al. 2011, fig. 2). The anomalous first ribs of *E. robustus* and *B. musculus* have
297 thin heads lacking distinct tuberculum and capitulum and their general shape clearly differs from
298 that of the first rib of MST Q1.

299 *Balaenoptera borealis* and *B. edeni*, the two extant balaenopterids having bifurcated first rib as
300 MST Q1, form a distinct clade in several phylogenies, both morphological (e.g. Bisconti et al., 2019)
301 and molecular (e.g. McGowen et al., 2020). Whiting *B. edeni* two subspecies, *B. edeni edeni* and *B.*
302 *edeni brydei*, are recognized, the latter sometimes considered a separate species (*B. brydei*) (Kato
303 and Perrin, 2018). Recently the new extant species *B. ricei*, belonging to the same *B. borealis*-
304 *B. edeni* clade, has been described (Rosel et al., 2021). *B. ricei* shares with *B. borealis* and *B. edeni*
305 the double-headed first rib (P. Rosel, pers. com. 2021).

306 Vertebrae. The unfused cervical vertebrae is a plesiomorphic condition shared by MST Q1 with
307 most mysticetes with the exception of the Balaenidae and *Caperea* (Neobalaenidae), having C1-C7
308 fusion (*Balaena*, *Eubalena*, *Caperea*) or C2-C7 fusion (*Antwerpibalaena*; Dubois de Lavignerie et

309 al., 2020). Actually, also in balaenopterids a fusion of the cervicals, although partial, can be present,
310 such as in *Balaenoptera physalus* with the first two-three cervicals sometimes fused, and in *B.*
311 *borealis* with a few cases with the first two cervicals fused (Tomlin, 1967). By contrast, completely
312 unfused C1-C7 have been reported for other balaenopterids (e.g. *Balaenoptera edeni*; Kato and
313 Perrin, 2018). Unfused C1-C7 has also been observed in the holotype and in the referred skeleton of
314 *Incakujira anillodefuego* (Marx and Kohno, 2016). It seems, therefore, that although in
315 balaenopterids unfused C1-C7 is the prevalent condition, two-three fused cervicals can be
316 sometimes observed in some species. Therefore a total non-fusion, as observed in MST Q1, cannot
317 be used as a diagnostic character, excepted to exclude its appurtenance to the Balaenidae or
318 Neobalaenidae.

319 The few information available from the poorly preserved vertebral column prevents an exhaustive
320 comparison of this part of the skeleton with that of other mysticetes. Nevertheless, measurements of
321 the centrum length (CL) taken on the broken vertebrae exposed on the calcarenite slab allowed the
322 pattern of CL from the second cervical to the last preserved caudal to be reconstructed, at least in
323 part. This CL pattern was graphed and compared with the CL patterns of some extant balaenopterids
324 (Fig. 7). Interesting, although incomplete, the CL pattern of MST Q1 exhibits a greater overlap with
325 the CL pattern of *Megaptera novaeangliae*, with an acute peak followed by an abrupt decrease in
326 the CL values. This peak represents the maximum length of the vertebrae and roughly corresponds,
327 in the extant balaenopterids, to the transition between the last lumbar to the first cervicals. The
328 similar CL patterns of *Balaenoptera musculus* and *B. physalus* clearly differ from MST Q1 for a
329 wider upper convexity and a less prominent and more centrally displaced peak. An intermediate
330 condition between *B. musculus* + *B. physalus* and the MST Q1 + *M. novaeangliae* is observed for
331 the similar patterns of *Balaenoptera borealis* and *B. edeni*. Finally, the pattern of *Balaenoptera*
332 *acutorostrata* differs from the one of MST Q1 mainly for the small number of vertebrae and for the
333 peak forming a more open angle. Despite these affinities between the CL pattern of MST Q1 with
334 *M. novaeangliae*, a general view of the curves plotted in the graph of figure 7 suggests that the CL

335 pattern could be linked to body size, being, for example, the patterns of *B. musculus* and *B. physalus*
336 very similar although the two largest whales are not closer to each other than to other congeners
337 (Marx and Kohno, 2016; McGowen et al., 2020). Therefore, considering the CL pattern as a
338 diagnostic character for mysticetes requires some caution.

339 Forelimb. The fragmentary right scapula of MST Q1 is poorly informative from a diagnostic point
340 of view, although the well preserved acromion represents a remarkable difference with *Megaptera*
341 *novaeangliae*, the only mysticete lacking of this process.

342 A comparison of the MSTQ1 humerus with that of other balaenopterids (Fig. 8), evidences a value
343 of its relative length ($b/a = 0.36$) near to the other species of *Balaenoptera* ($b/a = 0.37-0.33$) with *B.*
344 *acutorostrata* showing the lower value. The same value of MSTQ1 for this ratio is also observed in
345 “*Megaptera*” *hubachi*, whereas *Incakujira anillodefuego* and *Megaptera novaeangliae* exhibit more
346 elongated humeri ($b/a = 0.43$ and 0.43 respectively).

347 The MSTQ1 humerus is apparently slender than those of all other balaenopterid but this character
348 could be an artefact of the breakage and poor preservation of this bone. The head of the MSTQ1
349 humerus is relatively small ($c/b = 0.31$; Fig. 8), particularly if compared with *B. musculus* ($c/b =$
350 0.44) and *M. novaeangliae* ($c/b = 0.51$). The outlines of ulna and radius of MSTQ1 seem to be better
351 preserved than those of humerus, evidencing in this case a genuine slender and gracile shape of both
352 bones, similarly to *B. borealis* and *B. edeni* among the other balaenopterids. In this aspect the radius
353 and ulna of MST Q1 clearly differ from those significantly more robust of *B. acutorostrata*, *B.*
354 *musculus* and *I. anillodefuego*. The ulna and radius of *M. novaeangliae*, instead, differs from
355 MSTQ1 and from the other balaenopterid in their pronounced distal widening. The MSTQ1
356 olecranon process of the ulna is well developed both posteriorly and proximally as in all other
357 balaenopterids excepted *M. novaeangliae*, which have this process very reduced. In conclusion, the
358 whole shape of the MST Q1 forelimb is roughly similar to that of the extant rorqual species,
359 showing the better affinities with *B. borealis* and *B. edeni*.

360 Conclusive comparison remarks. Unfortunately, the incompleteness of the some diagnostic parts of

361 the MSTQ1 skeleton (e.g., the skull) dramatically limits the comparison with other mysticetes. The
362 most significant character observed in the MST Q1 skeleton is the bifurcated first rib, only known
363 in *Balaenoptera borealis*, *B. edeni*, and *B. ricei*. Such a shared character leads to the hypothesis that
364 MST Q1 belongs in the same clade of the three extant rorquals. Indeed, the morphology of the
365 tympanic bulla and forelimb bones of MST Q1 are compatible with both *B. borealis* and *B. edeni*,
366 but unfortunately it is not possible to confirm a closer affinity with one of these two species, due to
367 the limited diagnostic value and incompleteness of these bones. On the other hand, based of body
368 size estimation, MST Q1 was smaller than *B. edeni* and *B. borealis*, as confirmed by the relative
369 small size of the MST Q1 tympanic bulla. Rather, in body size MST Q1 is more similar to *B. ricei*
370 of which, however, the tympanic bulla is not sufficiently known for a detailed comparison (Rosel et
371 al., 2021, fig. S9d).

372 Regarding the small size, however, it should be remarked that the extant rorqual species include
373 several subspecies of reduced size, due to partial geographic segregation (e.g. the pygmy blue whale
374 *Balaenoptera musculus brevicauda*). Finally, MST Q1 differs from *B. edeni* and *B. borealis*, also for
375 the CL vertebral pattern, a character that in turn could be related to the smaller body size.

376 All the observations suggest that MST Q1 likely belong to an undescribed fossil species of
377 *Balaenoptera*, close to or nested in the *B. borealis*-*B. edeni*-*B. ricei* clade. So, pending the discovery
378 of a more complete specimen, MST Q1 is assigned to *Balaenoptera* sp.

379

380 **4. Taphonomy**

381 4.1. *Descriptive taphonomy*

382 A significant part of the preserved bones is articulated whereas the disarticulated bones are closely
383 associated near their anatomical position as, for example, most of the thoracic vertebrae, the ribs and
384 the forelimb bones (Fig. 2). The completeness degree of skeleton is moderately high, with the missing
385 bones being the hyoids, the atlas, some thoracics, about one meter of the posterior portion of the

386 column (i.e. the last about 10 caudals), the sternal bones, and some forelimb bones (left scapula and
387 most of hand bones), and the destroyed portion of the cranium. However, some of these missing bones
388 could be still fully embedded in the matrix and not visible on the upper surface of the calcarenite slab,
389 or to have been destroyed during the canal excavation.

390 The analysis of the bones preservation has been partially compromised by the recent damage due to
391 the excavation that, for example, destroyed about the half dorsal portion of most of the vertebrae.
392 However, even some bones that do not appear to have suffered evident recent damage (e.g. the
393 forelimb bones), show some fractures, breakages and deformations.

394

395 4.2. *Shark bite marks*

396 The exposed surface of the seventh? right rib is affected by at least five subparallel 5-10 mm long
397 marks identified as shark bites (Fig. 9A), in particular as type 1 marks, produced by a tooth impacting
398 the surface of the bone from the above downward (Cigala Fulgosi, 1990; Bianucci et al., 2010).
399 However, due to the bad preservation of the cortical bone surface, it was not possible to establish
400 whether marks were produced by unserrated or serrated teeth and therefore is not possible to
401 speculate on shark species .

402

403 4.3. *Associated fauna*

404 A *Carcharodon carcharias* tooth was found near the end of the fourth left rib and in close proximity
405 of the isolated right phalanx (Fig. 9B).

406 The embedding calcarenite contains scarce benthic invertebrate macrofauna, consisting only of
407 bivalves and gastropod shells, preserved as external and internal moulds. Some of these molluscan
408 remains were found in the same horizon and strictly associated to the whale skeleton. Among the
409 bivalves, articulated *Acanthocardia echinata* and molds of articulated *Anodontia* cf. *fragilis* were
410 found between mandibles and between the second? and third? right ribs. Molds of *A.* cf. *fragilis* are
411 also seen near the fifth left rib and between the left radius and the left ulna. An articulated specimen

412 of *Venus nux* (as external mold) apparently is in life position (about 45° with respect to vertical),
413 between the epiphysis and the respective centrum of one of the first lumbar (Fig. 9C). Among the
414 gastropods, a mold of *Gibbula magus* was found ca 40 cm posterior to the last preserved left ribs.

415

416 4.4. Reconstruction of the taphonomic history

417 The high degree of skeletal articulation and completeness of MST Q1 suggests a limited or absence
418 of refloating of the carcass after falling. In fact, during a long refloating phase a whale carcass
419 gradually dismembers due to decay and scavenging, with mandibles, cranium, tail, and forelimbs fall
420 to the bottom (Schäfer, 1972). According to Allison et al. (1991), the permanence of a whale carcass
421 on the seafloor depends on the hydrostatic pressure, temperature and on the interplay between two
422 main biological factors: production of decomposition gas and rate of scavenging. Decomposition can
423 produce a volume of gas sufficient to bloat and refloat the carcass if not previously partially
424 dismembered and if the hydrostatic pressure (and consequently the depth) is not too strong (Smith et
425 al., 2015; Moore et al., 2020). The depth preventing the refloating was estimated 1000 m by Allison
426 et al. (1991) and successively reduced by Reisdorf et al. (2012) who reported that whale carcasses
427 “may rise from water depths up to 50 m, but never from below 100 m”. A proxy for palaeodepth
428 inference is provided by the associated molluscan assemblage, which suggests a mid-shelf setting
429 near to the boundary between infralittoral and circalittoral environment, probably 40-60 m. In
430 particular, the bivalves *Acanthocardia echinata* and *Venus nux* are shallow burrowers in sandy-muddy
431 bottoms (Poutiers, 2016; Tirado et al., 2011), and are common components of Plio-Pleistocene shelf
432 assemblages (Spano, 1989; Moshkovitz, 2012; Crippa and Raineri, 2015). The rising of the whale
433 carcass from such a shallow depth may have been prevented by early scavenger action suggested by
434 the occurrence of a *Carcharodon carcharias* tooth near a phalanx and by shark bite marks on a rib.
435 Scavenging during initial flotation, or soon after sinking, would have favoured a fast removal of
436 abdominal tissues, thus reducing the accumulation of decomposition gasses. The partial
437 disarticulation of the thoracic region could be related to shark scavenging, together with collapse of

438 the rib cage due to decay. The occurrences of shark bite marks on the bones and shark teeth in
439 association with fossil whales are well documented, testifying both predation and scavenging
440 activities (Deméré and Cerutti, 1982; Cigala Fulgosi, 1990; Bianucci et al., 2000, 2010, 2018;
441 Collareta et al., 2017; Bosio et al., 2021). Interestingly, the extant great white sharks do not actively
442 prey on baleen whales but rather feed on their floating carcasses, showing initial preference for the
443 tail and the blubber-rich regions (Long and Jones, 1996; Curtis et al., 2006; Fallws et al., 2013). The
444 lack of tail on the MST Q1 skeleton, the shark bite marks and the *C. carcharias* tooth, both found in
445 the fat abdominal region, supports a scavenging action.

446 The occurrence of the bivalve *Anodontia fragilis* in the molluscan assemblage could testify the
447 development of a sulphophilic stage, usually following mobile-scavenger and enrichment-opportunist
448 stages during the development of a whale fall community (Smith et al., 2002, 2014; Danise et al.,
449 2010; Danise and Dominici, 2014). *A. fragilis* is a representative of the Lucinidae, one of the bivalve
450 families known to host chemosynthetic bacteria (Taylor and Glover, 2005; 2006; Duperron et al.,
451 2013). Chemosymbiotic bivalves are components of recent (Smith and Baco, 2003) and fossil
452 (Amano and Little, 2005; Dominici et al., 2009; Danise et al., 2010) whale fall communities during
453 the sulphophilic stage (Smith et al., 2002, 2014). Finally, the presence of non-chemosymbiotic
454 molluscs close to the skeleton , such as *Venus nux*, suggests its colonization during the following reef
455 stage (Smith et al., 2002, 2014).

456

457 **5. Paleobiogeography**

458 *5.1. The Mediterranean Pleistocene baleen whale fauna*

459 The attribution of the MST Q1 skeleton to *Balaenoptera* sp. within the *B. borealis*-*B. edeni*-*B. ricei*
460 clade provides new data on the still poorly known Pleistocene cetacean fauna of the Mediterranean
461 Sea. In particular, the Mediterranean Pleistocene fossil record of mysticetes until now was mainly
462 represented by two finds: a large skeleton referred to *Balaenoptera* cf. *musculus* from the Lower

463 Pleistocene (1.5–1.25 Ma) of Matera, southern Italy (Bianucci et al., 2019), and an isolated tympanic
464 bulla referred to cf. *Caperea* sp. (Neobalaenidae) from the Lower Pleistocene (1.9–1.7 Ma) of Sicily
465 (Tsai et al., 2017). Furthermore, indirect evidences provided by the study of fossil whale barnacles
466 from Salento Peninsula and Sicily (South Italy) suggested a breeding/calving area in the
467 Mediterranean during the Early Pleistocene for at least a balaenopterid belonging or closely related
468 to *Megaptera* and a balaenid belonging or closely related to *Eubalaena* (Collareta et al. 2016,
469 2018a,b). In summary, by adding the new balaenopterid here described, during the Early Pleistocene
470 two rorquals (*Balaenoptera* cf. *musculus* and *Balaenoptera* sp.), one humpback whale (*Megaptera*?),
471 one right whale (*Eubalaena*?), and one pygmy right whale (cf. *Caperea* sp.) swam in the
472 Mediterranean. This baleen whale assemblage shows a high disparity evidenced by the significant
473 differences in morphology and size (from the ca 26 m in length of *B.* cf. *musculus* to the 5-6 m of cf.
474 *Caperea* sp.).

475

476 5.2. The modern Mediterranean baleen whale fauna

477 The present-day mysticete community of the Mediterranean contrasts dramatically with the Early
478 Pleistocene scenario. Indeed, today the fin whale *Balaenoptera physalus* is the only mysticete that
479 regularly frequents the Mediterranean (Notarbartolo-Di-Sciara et al., 2003). However, the *B. physalus*
480 distribution in the Mediterranean is not uniform, e.g. it is regularly present in the relatively cool and
481 productive northwestern Mediterranean while it is rarer and not regularly present in the Adriatic Sea
482 (Notarbartolo-Di-Sciara et al., 2003). Concerning other baleen whales reported in the Mediterranean
483 occasionally, *Balaenoptera acutorostrata*, and *Megaptera novaeangliae* are considered visitor
484 species, being their record represented by a few individuals from North Atlantic populations
485 occasionally entered in the Mediterranean (Reeves and Notarbartolo di Sciara, 2006; Notarbartolo di
486 Sciara and Birkun, 2010; Russo et al., 2016). Two other baleen whales, *Balaenoptera borealis* and
487 *Eubalaena glacialis* are considered vagrant species, being only recorded with five and two specimens
488 respectively in the Mediterranean (Reeves and Notarbartolo di Sciara, 2006; Notarbartolo di Sciara

489 and Birkun, 2010). In particular, *B. borealis* is a cosmopolitan species preferring temperate and
490 subpolar waters (Gambell, 1985; Horwood 1987) and it does not seem to usually enter the semi-
491 enclosed basins (Reeves et al., 1998). Its Mediterranean records are limited to the northwestern coasts
492 (two reports in Spain and three in France) (Notarbartolo di Sciara and Birkun, 2010).

493

494 5.3. Palaeoceanographic changes as keys to understand the Mediterranean Pleistocene baleen whale 495 diversity and disparity

496 Recent studies indicate that the intensification of glacial-interglacial phases and an high interchanges
497 between the two hemispheres were the main drivers to shape the biological distribution of whales,
498 during the Quaternary (Tsai et al., 2017; Tsai and Chang, 2019). In the Mediterranean, beginning
499 since the late Piacenzian, the teleostean fauna records an increasing number of Atlantic taxa, including
500 several subpolar and temperate taxa that spread into the central and eastern Mediterranean sectors as
501 a consequence of climatic deterioration and oceanographic changes (Girone et al., 2006; Agiadi et al.,
502 2011; 2018). The importance of the Atlantic faunistic flow increased during the Gelasian and went
503 on throughout Middle and Late Pleistocene. In analogy, we can hypothesize that climate variability
504 and related oceanographic changes in terms of temperatures and nutrients have driven the dispersal
505 of oceanic baleen whales from the North Atlantic to the Mediterranean. The Pleistocene southern Italy
506 paleogeography could have also played a role in the baleen whale frequentation of the Adriatic, which
507 today is not regularly inhabited by *Balaenoptera physalus*. At least since the beginning of Pleistocene
508 (about 2.5 Ma ago), this Mediterranean sector was affected by subsidence that caused the drowning
509 of most of the Apulian peninsula, giving origin to a vast archipelago (Tropeano and Sabato, 2000;
510 Tropeano et al., 2002a; 2002b; 2018). The widest and deepest seaway was the Bradanic Trough,
511 connecting Adriatic Sea with Ionian Sea (Tropeano et al., 2018) (Fig. 1B). High productivity could
512 have favoured the arrival of *Balaenoptera* sp. in the Adriatic through the Sicily Channel. This route
513 probably followed the path of the Modified Atlantic Waters (MAW) entering through the Strait of
514 Gibraltar and flowing eastward (Fig. 1A). The influx of MAW into the Ionian basin originated

515 upwelling events and nutrients supply at the periphery of an anticyclonic gyre along the south Italian
516 coasts before reaching the south Adriatic Sea (Civitarese et al., 2010). The strengthening of the
517 Atlantic Ionian Stream jet, during more arid and colder conditions, shifts towards the north the
518 influence of Atlantic waters (Poulain et al., 2012) that enter in the northern area of the Ionian Sea. It
519 cannot be excluded that the influence of productive waters at the studied site was reinforced through
520 the Bradanic Trough seaway during Pleistocene (Fig. 1B). This condition is in line with the modern
521 distribution of the fin whale in the Mediterranean, mainly occurring in deep water, as well as in slope
522 and shelf waters with coastal upwelling and high concentration of zooplankton (Notarbartolo di Sciara
523 et al., 2003; Notarbartolo di Sciara and Birkun, 2010).

524

525 **Conclusions**

526 Although MST Q1 represents one of most complete cetacean skeletons from Pleistocene ever
527 found, its skull, the most diagnostic anatomical part for neocetes, is strongly damaged leading its
528 systematic assignment rather complicated. However, after a detailed comparison MST Q1 is here
529 referred to a possible undescribed fossil species of *Balaenoptera* close to or nested in the clade
530 formed by *B. borealis*, *B. edeni* and *B. ricei*, three extant species sharing with MST Q1 the
531 bifurcated first rib. Nevertheless, the scarcity of significative diagnostic characters suggests a
532 prudent assignation of MST Q1 to *Balaenoptera* sp.

533 The high degree of skeletal articulation and completeness supports a limited or absent refloating of
534 the carcass after falling, whereas the associated molluscs suggest that it settled at a deep of 40-60 m.
535 Rising of the whale carcass from such a shallow depth may have been prevented by early scavenger
536 action suggested by the associated *Carcharodon carcharias* tooth and by the shark bite marks. The
537 associated bivalve *Anodontia fragilis* could testify the development of a sulphophilic stage, whereas
538 non-chemosymbiotic molluscs, such as *Venus nux*, indicate the colonization of the skeleton in the
539 subsequent reef stage.

540 The Bari skeleton here described provides new data for the knowledge of the Pleistocene mysticete
541 fauna of the Mediterranean, so far known on very few remains and indirect evidences from baleen
542 whale barnacles. In particular, this whale fauna included at least two rorquals (*Balaenoptera* cf.
543 *musculus* and *Balaenoptera* sp.) and one pygmy right whale (cf. *Caperea* sp.) based on skeletal
544 remains, plus one humpback whale (*Megaptera*?) and one right whale (*Eubalaena*?) based baleen
545 whale barnacles. This scenario contrasts with the current mysticete community of the
546 Mediterranean, only represented, considering the regular species, by the fin whale *Balaenoptera*
547 *physalus*.

548 A possible key to understand the greater diversity and disparity of the Mediterranean baleen whale
549 assemblage in the Pleistocene in respect to the present could be the paleoclimatic, oceanographic
550 and geodynamic changes, and related reassessment of the distribution of nutrients, causing dispersal
551 processes of these cetaceans from the North Atlantic to the Mediterranean and, within the
552 Mediterranean, from west to the southern Adriatic Sea.

553 Future discoveries in southern Italy, where Pleistocene marine deposits are widely exposed, could
554 allow a better definition of this still fragmentary picture of the Quaternary whale fauna of the
555 Mediterranean.

556

557

558 **Author contributions**

559 Andrea Zazzera, Angela Girone and Giovanni Bianucci: Data curation, Formal analysis,
560 Investigation, Methodology, Conceptualization, Writing - original draft; Reviewing and Editing.

561 Rafael La Perna: Conceptualization, Investigation, Formal analysis, Original draft preparation

562 Maria Marino: Conceptualization, Formal analysis

563 Patrizia Maiorano: Conceptualization, Formal analysis

564 Raffaele Sardella: Conceptualization, Original draft preparation

565 Vincenza Montenegro: Conceptualization

566 Ruggero Francescangeli: Conceptualization

567

568 **Declaration of competing interest**

569 The authors declare that they have no known competing financial interests or personal relationships
570 that could have appeared to influence the work reported in this paper.

571

572 **Acknowledgments**

573 We are grateful to P. Agnelli, S. Farina, R. Salas-Gismondi, C. Lefèvre, G. Lenglet, J. G. Mead, J. J.
574 Ososki, C. Potter, and S. van der Mije for facilitating the access to the skeletal collections of
575 modern baleen whales under their care. Special thanks to F.G. Marx for useful discussions about the
576 systematics of baleen whales. This research was financially supported by Università degli Studi di
577 Bari Aldo Moro, Fondi di Ateneo P. Maiorano, 2018 and benefited of instrumental upgrades from
578 “Potenziamento Strutturale PONa3_00369 dell'Università degli Studi di Bari, Laboratorio per lo
579 Sviluppo Integrato delle Scienze e delle Tecnologie dei Materiali Avanzati e per dispositivi
580 innovativi (SISTEMA)”.

581

582 **References**

- 583 Agiadi, K., Triantaphyllou, M., Girone, A., Karakitsios, V., 2011. The early Quaternary
584 palaeobiogeography of the eastern Ionian deep-sea Teleost fauna: a novel palaeocirculation
585 approach. *Palaeogeography, Palaeoclimatology, Palaeoecology* 306, 228–242.
586 <https://doi.org/10.1016/j.palaeo.2011.04.029>
- 587 Agiadi, K., Girone, A., Koskeridou, E., Moissette, P., Cornée, J.-J., Quillévéré, F., 2018. Pleistocene
588 marine fish invasions and paleoenvironmental reconstructions in the eastern Mediterranean.
589 *Quaternary Science Reviews* 196, 80–99. <https://doi.org/10.1016/j.quascirev.2018.07.037>

590 Allison, P.A., Smith, C.R., Kukert, H., Deming, J.W., Bennett, B.A., 1991. Deep-water taphonomy
591 of vertebrate carcasses: a whale skeleton in the bathyal Santa Catalina Basin. *Paleobiology* 17,
592 78–89.<https://doi.org/10.1017/S0094837300010368>

593 Amano, K., Little, C.T.S., 2005. Miocene whale-fall community from Hokkaido, northern Japan.
594 *Palaeogeography, Palaeoclimatology, Palaeoecology* 215, 345–
595 356.<https://doi.org/10.1016/j.palaeo.2004.10.003>

596 Andrews, R.C., 1916. Monographs of the Pacific Cetacea, II. The sei whale (*Balaenoptera borealis*
597 Lesson), history, habits, external anatomy, osteology, and relationship. *Memoirs of the American*
598 *Museum of Natural History, New Series* 1, 291-388, pls, XXIX-XLII.

599 Bianucci, G., 2014. I cetacei fossili nei musei italiani. *Museologia Scientifica, Memorie* 13, 7-17.
600 <http://www.anms.it/upload/rivistefiles/8756659e2760a918a73208e32ad8ddf0.pdf>

601 Bianucci, G., Bisconti, M., Landini, W., Storai, T., Zuffa, M., Giuliani, S., Mojetta, A., 2000.
602 Trophic interaction between white shark, *Carcharodon carcharias*, and cetaceans: a comparison
603 between Pliocene and Recent data from Central Mediterranean Sea. In: Vacchi M., La Mesa G.,
604 Serena F., Séret B. (Eds.). *Proceedings of the IV European Elasmobranch Association Meeting*, pp.
605 33–48.

606 Bianucci, G., Collareta, A., Bosio, B., Landini, W., Gariboldi, K., Gioncada, A., Lambert, O.,
607 Malinverno, E., Muizon, C. de, Varas-Malca, R., Villa, I.M., Coletti, G., Urbina, M., Di Celma,
608 C., 2018. Taphonomy and palaeoecology of the lower Miocene marine vertebrate assemblage of
609 Ullujaya (Chilcatay Formation, East Pisco Basin, southern Peru). *Palaeogeography,*
610 *Palaeoclimatology, Palaeoecology* 511, 256-279.<https://doi.org/10.1016/j.palaeo.2018.08.013>

611 Bianucci, G., Marx, F.G., Collareta, A., Di Stefano, A., Landini, W., Morigi, C., Varola, A., 2019.
612 Rise of the titans: baleen whales became giants earlier than thought. *Biology Letters* 15,
613 20190175.<https://doi.org/10.1098/rsbl.2019.0175>

614 Bianucci, G., Sorce, B., Storai, T., Landini, W., 2010. Killing in the Pliocene: shark attack on a
615 dolphin from Italy. *Palaeontology* 53, 457–470. <http://dx.doi.org/10.1111/j.1475->

616 4983.2010.00945.x

617 Bisconti, M., 2006. *Titanocetus*, a new baleen whale from the middle Miocene of northern Italy
618 (Mammalia, Cetacea, Mysticeti). *Journal of Vertebrate Paleontology* 26, 344-
619 354. [https://doi.org/10.1671/0272-4634\(2006\)26\[344:TANBWF\]2.0.CO;2](https://doi.org/10.1671/0272-4634(2006)26[344:TANBWF]2.0.CO;2)

620 Bisconti, M., 2009. Taxonomy and evolution of the Italian Pliocene Mysticeti (Mammalia,
621 Cetacea): a state of the art. *Bollettino della Società Paleontologica Italiana* 48, 147–156.
622 http://paleoitalia.org/media/u/archives/09_Bisconti.pdf

623 Bisconti, M., 2010. A new balaenopterid whale from the late Miocene of the Stirone River, Northern
624 Italy (Mammalia, Cetacea, Mysticeti). *Journal of Vertebrate Paleontology* 30, 943-958.
625 <https://doi.org/10.1080/02724631003762922>

626 Bisconti, M, Munsterman, DK, Post, K., 2019. A new balaenopterid whale from the late Miocene of
627 the Southern North Sea Basin and the evolution of balaenopterid diversity (Cetacea, Mysticeti).
628 *PeerJ* 7: e6915 DOI 10.7717/peerj.6915

629 Bisconti M., Damarco P., Selina M., Pavia M., Carnevale G. 2021. The earliest baleen whale from
630 the Mediterranean: large-scale implications of an early Miocene thalassotherianmysticete from
631 Piedmont, Italy. *Papers in Palaeontology* 7, 1147-1166. doi: 10.1002/spp2.1336

632 Bosio G., Collareta A., Di Celma C., Lambert O., Marx F.G., Muizon C. de, Gioncada A., Gariboldi
633 K., Malinverno E., Varas-Malca R., Urbina M., Bianucci G. 2021. Taphonomy of marine
634 vertebrates of the Pisco Formation (Miocene, Peru): Insights into the origin of an outstanding
635 Fossil-Lagerstätte. *PLOS ONE*.doi: 10.1371/journal.pone.0254395

636 Buchholtz, E., A., 2011. Vertebral and rib anatomy in *Caperea marginata*: implications for
637 evolutionary patterning of the mammalian vertebral column. *Marine Mammal Science* 27(2),
638 382–397. <https://doi.org/10.1111/j.1748-7692.2010.00411.x>

639 CigalaFulgosi, F., 1990. Predation (or possible scavenging) by a great white shark on an extinct
640 species of bottlenosed dolphin in the Italian Pliocene. *Tertiary Research* 12, 17–36.

641 Civitarese, G., Gačić, M., Lipizer, M., EusebiBorzelli, G. L., 2010. On the impact of the Bimodal

642 Oscillating System (BiOS) on the biogeochemistry and biology of the Adriatic and Ionian Seas
643 (Eastern Mediterranean), *Biogeosciences* 7, 3987–3997. doi:10.5194/bg-7-3987-2010

644 Collareta, A., Margiotta, S., Varola, A., Catanzariti, R., Bosselaers, M., Bianucci, G., 2016. A new
645 whale barnacle from the early Pleistocene of Italy suggests an ancient right whale breeding
646 ground in the Mediterranean. *Comptes Rendus Palevol* 15, 473-481.
647 <https://doi.org/10.1016/j.crpv.2015.10.006>

648 Collareta, A., Insacco, G., Reitano, A., Catanzariti, R., Bosselaers, M., Montes, M., Bianucci, G.,
649 2018a. Fossil whale barnacles from the lower Pleistocene of Sicily shed light on the coeval
650 Mediterranean cetacean fauna. *Carnets de Geologie* 18 (2), 9-22. doi: 10.4267/2042/65747

651 Collareta, A., Regattieri, E., Zanchetta, G., Lambert, O., Catanzariti, R., Bosselaers, M., Covelo, P.,
652 Varola, A., Bianucci, G., 2018b. New insights on ancient cetacean movement patterns from
653 oxygen-isotope analyses of a Mediterranean Pleistocene whale barnacle. *Neues Jahrbuch für*
654 *Geologie und Paläontologie Abhandlungen* 288, 143 –159. doi:10.1127/njgpa/2018/0729

655 Collareta, A., Collareta, M., Berta, A., Bianucci, G., 2020. On Leonardo and a fossil whale: a
656 reappraisal with implications for the early history of palaeontology. *Historical Biology* doi:
657 10.1080/08912963.2020.1787403

658 Collareta, A., Lambert, O., Landini, W., Di Celma, C., Malinverno, E., Varas-Malca, R., Urbina, M.,
659 Bianucci, G., 2017. Did the giant extinct shark *Carcharocles megalodon* target small prey?
660 Bitemarks on marine mammal remains from the late Miocene of Peru. *Palaeogeography,*
661 *Palaeoclimatology, Palaeoecology* 469, 84-91. <https://doi.org/10.1016/j.palaeo.2017.01.001>

662 Cozzi, B., Podestà, M., Mazzariol, S., Zotti, A., 2012. Fetal and early post-natal mineralization of
663 the tympanic bulla in fin whales may reveal a hitherto undiscovered evolutionary trait. *PLoS*
664 *ONE* 7(5): e37110. doi:10.1371/journal.pone.0037110

665 Crippa, G., Ranieri, G., 2015. The genera *Glycymeris*, *Aequipecten* and *Arctica*, and associated
666 mollusk fauna of the Lower Pleistocene Arda River section (northern Italy). *Rivista Italiana di*
667 *Paleontologia e Stratigrafia* 121 (1), 61-101. Doi: <https://doi.org/10.13130/2039-4942/6401>

668 Curtis, T.H., Kelly, J.T., Menard, K.L., Laroche, R.K., Jones, R.E., Klimley, A.P., 2006.
669 Observations on the behavior of white sharks scavenging from a whale carcass at Point Reyes,
670 California. *California Fish and Game* 92(3), 113-124.
671 <https://nrm.dfg.ca.gov/FileHandler.ashx?DocumentID=47405&inline=1>

672 Danise, S., Dominici, S., 2014. A record of fossil shallow-water whale falls from Italy. *Lethaia* 47,
673 229–243. <https://doi.org/10.1111/let.12054>

674 Danise, S., Dominici, S., Betocchi, U., 2010. Mollusk species at a Pliocene shelf whale fall
675 (Orciano Pisano, Tuscany). *Palaios* 25, 449–556. <https://doi.org/10.2110/palo.2009.p09-139r>

676 Deméré, T.A., Cerutti, R.A., 1982. A Pliocene shark attack on a cethotheriid whale. *Journal of*
677 *Paleontology* 56 (6), 1480–1482.

678 Dominici, S., Cioppi, E., Danise, S., Betocchi, U., Gallai, G., Tangocci, F., Valleri, G., Monechi, S.,
679 2009. Mediterranean fossil whale falls and the adaptation of mollusks to extreme habitats.
680 *Geology* 37, 815–818. <https://doi.org/10.1130/G30073A.1>

681 Dominici, S., Danise, S., Cau, S., Freschi, A., 2020. The awkward record of fossil whales. *Earth-*
682 *Science Reviews* 205, 103057. <https://doi.org/10.1016/j.earscirev.2019.103057>

683 Dubar, J., 1828. *Ostéographie de la baleine échouée à l'est du port d'Ostende, le 4 novembre 1827;*
684 *précédée d'une notice sur la découverte et la dissection de ce Cétacée.* Laurent Frères,
685 Imprimeurs-Libraires: Bruxelles. 61, 13 folded plates pp.

686 Duboys de Lavigerie, G., Bosselaers, M., Goolaerts, S., Park, T., Lambert, O., Marx, F.G., 2020.
687 New Pliocene right whale from Belgium informs balaenid phylogeny and function. *Journal of*
688 *Systematic Palaeontology* 18/14, 1141–1166. <https://doi.org/10.1080/14772019.2020.1746422>

689 Duperron, S., Gaudron, S.M., Rodrigues, C.F., Cunha, M.R., Decker, C., Olu, K., 2013. An
690 overview of chemosynthetic symbioses in bivalves from the North Atlantic and Mediterranean
691 Sea. *Biogeosciences* 10, 3241–3267. <https://doi.org/10.5194/bg-10-3241-2013>, 2013.

692 Ekdale, E.G., Berta, A., Deméré, T.A., 2011. The comparative osteology of the petrotympanic
693 complex (ear region) of extant baleen whales (Cetacea: Mysticeti). *PLoS ONE*, 6(6), e21311.

694 doi:10.1371/journal.pone.0021311

695 Evans, H.E., de Lahunta, A., 2013. Miller's anatomy of the dog, 4th edn. St. Louis: Elsevier
696 Saunders.

697 Fallows, C., Gallagher, A.J., Hammerschlag, N., 2013. White Sharks (*Carcharodon carcharias*)
698 scavenging on whales and its potential role in further shaping the ecology of an apex predator.
699 PLoS ONE 8(4): e60797. <https://doi.org/10.1371/journal.pone.0060797>

700 Galatius, A, Kinze, CC., 2003. Ankylosis patterns in the postcranial skeleton and hyoid bones of the
701 harbour porpoise (*Phocoenaphocoena*) in the Baltic and North Sea. Canadian Journal of Zoology
702 – Revue Canadienne de Zoologie 81, 1851–1861. <https://doi.org/10.1139/z03-181>

703 Gambell, R., 1985. Sei whale *Balaenoptera borealis* Lesson, 1828. Pp. In: S.H. Ridgway and R.
704 Harrison (eds). Handbook of marine mammals 3, 155-170. Academic Press, London

705 Girone, A., Nolf, D., Cappetta, H., 2006. Pleistocene fish otoliths from the Mediterranean basin: a
706 synthesis. Geobios, 39, 651–671. <https://doi.org/10.1016/j.geobios.2005.05.004>

707 Horwood, J., 1987. The sei whale: population biology, ecology and management. Croom Helm, 375
708 pp.

709 Kato, H., Perrin, W.F., 2018. Bryde's whales: *Balaenoptera aedeni/brydei*. In: Würsig, B., Theewissen,
710 J.G.M., Kovacs, K.M. (eds). Encyclopedia of Marine Mammals (Third Edition). Academic Press:
711 London, pp. 158–163.

712 Kato, H., 1988. Ossification pattern of the vertebral epiphyses in the southern minke whale.
713 Scientific Report Whales Research Institute 39, 11-19.

714 Kemper, C.M., Leppard, P., 1999. Estimating body length of pygmy right whales
715 (*Caperea marginata*) from measurements of the skeleton and baleen. Marine Mammal Science
716 15(3), 683-700. <https://doi.org/10.1111/j.1748-7692.1999.tb00836.x>

717 Kinze M.A.C., 2005. Re-identification of a skeleton of the Bryde's whale (*Balaenoptera aedeni*) from
718 the northern coast of Borneo. Natural History Bulletin of the Siam Society 53, 133–144.
719 <https://www.thaiscience.info/journals/Article/NHB/10439469.pdf>

720 Lambert, O., Bianucci, G., Post, K., de Muizon, C., Salas-Gismondi, R., Urbina, M., Reumer, J.,
721 2010. The giant bite of a new raptorial sperm whale from the Miocene epoch of Peru. *Nature*
722 466(7302), 105-108. <https://doi.org/10.1038/nature09067>

723 Long, D.J., Jones, R.E., 1996. White shark predation and scavenging on cetaceans in the eastern
724 North Pacific Ocean. In: Klimley, A.P., Ainley, D.G. (Eds.). *Great White Sharks: the Biology of*
725 *Carcharodon carcharias*. Academic Press, San Diego, pp. 293–307.

726 Marx, F.G., Kohno, N., 2016. A new Miocene baleen whale from the Peruvian desert. *Royal Society*
727 *Open Science* 3, 160542. <https://doi.org/10.1098/rsos.160542>

728 Marx, F.G., Lambert, O., Uhen, M.D., 2016. *Cetacean Paleobiology* (1st Ed). John Wiley & Sons,
729 Chichester, U.K, 319 pp.

730 McGowen, M.R., Tsagkogeorga, G., Álvarez-Carretero, S., dos Reis, M., Struebig, M., Deaville, R.,
731 Jepson, P.D., Jarman, S., Polanowski, A., Morin, P.A., Rossiter, S.J., 2020. Phylogenomic
732 Resolution of the cetacean tree of life using target sequence capture. *Systematic Biology* 69, 3,
733 479–501. <https://doi.org/10.1093/sysbio/syz068>

734 Mead, J.G., Fordyce, R.E., 2009. The therian skull: a lexicon with emphasis on the odontocetes.
735 *Smithsonian Contributions to Zoology* 249 pp. <https://doi.org/10.5479/si.00810282.627>

736 Montenegro, V., 2016. “I giorni della Balena”. Una storia per la valorizzazione del fossile di
737 balenottera del Museo di Scienze della Terra dell’Università degli Studi di Bari.
738 *Museologia Scientifica* 10, 165-171.

739 Moore, M.J., Mitchell, G.H., Rowles, T.K., Early, G., 2020. Dead cetacean? beach, bloat, float,
740 sink. *Frontiers in Marine Science* 7, 333. doi: 10.3389/fmars.2020.00333

741 Moshkovitz, S., 2012. The Mollusca in the marine Pliocene and Pleistocene sediments of south-
742 eastern Mediterranean basin (Cyprus-Israel). Ministry of Energy and Water Resources,
743 Geological Survey of Israel, Report GSI/25/2012, 106 pp.

744 Nishiwaki, M., Kasuya T., 1971. Osteological note of an Antarctic sei whale *Scientific Report*
745 *Whales Research Institute* 23, 83-89.

- 746 Notarbartolo di Sciara, G., Birkun, A.Jr., 2010. Conserving whales, dolphins and porpoises in the
747 Mediterranean and Black Seas. ACCOBAMS status report, 2010. *ACCOBAMS*, Monaco, 212 pp.
- 748 Notarbartolo di Sciara, G., Zanardelli, M., Jahoda, M., Panigada, S., Airoidi, S., 2003. The fin
749 whale *Balaenopteryphysalus* (L. 1758) in the Mediterranean Sea. *Mammal Review*, 33, 105–
750 150. doi:10.1046/j.1365-2907.2003.00005.x
- 751 Omura, H., 1959. Bryde's whale from the coast of Japan. *Scientific Report Whales Research*
752 *Institute* 14, 1-33.
- 753 Omura, H., Kasuya, T., Kato, H., Wada, S., 1981. Osteological study of the Bryde's whale from the
754 central South Pacific and eastern Indian Ocean. *Scientific Reports of the Whales Research*
755 *Institute* 33, 1–26.
- 756 Pieri, P., Sabato, L., Spalluto, L., Tropeano, M., 2011. Note illustrative della carta geologica
757 dell'area urbana di Bari in scala 1:25.000. *Rendiconti Online della Società Geologica Italiana* 14,
758 26-36. doi: 10.3301/ROL.2011.04
- 759 Poulain, P.M., Menna, M., Mauri, E., 2012. Surface geostrophic circulation of the Mediterranean
760 Sea derived from drifter and satellite altimeter data. *Journal of Physical Oceanography* 42 (6),
761 973–990. <https://doi.org/10.1175/JPO-D-11-0159.1>
- 762 Poutiers, J.M., 2016. Bivalves (Acephala, Lamellibranchia, Pelecypoda). In: Carpenter K.E. and De
763 Angelis N. (eds.). *The living marine resources of the Eastern Central Atlantic. Volume 2.*
764 *Bivalves, gastropods, hagfishes, sharks, batoid fishes, and chimaeras. FAO Species Identification*
765 *Guide for Fishery Purposes*, Rome, FAO. pp. 665–1509.
- 766 Pyenson, N.D., Goldbogen, J.A., Shadwick, R.E., 2013. Mandible allometry in extant and fossil
767 *Balaenopteridae* (Cetacea: Mammalia): the largest vertebrate skeletal element and its role in
768 rorqual lunge feeding. *Biological Journal of the Linnean Society* 108 (3), 586–
769 599. <https://doi.org/10.1111/j.1095-8312.2012.02032>
- 770 Reeves, R.R., Notarbartolo Di Sciara, G., 2006. *The status and distribution of cetaceans in the*
771 *Black sea and Mediterranean Sea. IUCN Centre for Mediterranean Cooperation*, Malaga, Spain.

772 137 pp. <http://www.iucn-csg.org/wp-content/uploads/2010/03/ReevesNotarbartolo2006.pdf>

773 Reeves, R., Silber, G., Payne, M., 1998. Draft recovery plan for the fin whale *Balaenopteraphysalus*
774 and seiwhale *Balaenoptera borealis*. Silver Spring, Maryland: National Marine Fisheries
775 Service, 66 pp.

776 Reisdorf, A.G., Roman, B., Wyler, D., Benecke, M., Klug, C., Maisch, M., Fornaro, P., Wetzel, A.,
777 2012. Float, explode or sink: postmortem fate of lung-breathing marine vertebrates.
778 *Palaeobiodiversity and Palaeoenvironments* 92, 67–81. <http://dx.doi.org/10.1007/s12549-011->
779 0067-z

780 Rio, D., Raffi, I., Villa, G., 1990. Pliocene-Pleistocene calcareous nannofossil distribution patterns
781 in the Western Mediterranean, in: *Proceedings of the Ocean Drilling Program. Scientific Results.*
782 *Ocean Drilling Program*, College Station, TX, pp. 513–533

783 Rosel, P.E., Wilcox, L.A., Yamada, T.K., Mullin, K.D., 2021. A new species of baleen whale
784 (*Balaenoptera*) from the Gulf of Mexico, with a review of its geographic distribution. *Marine*
785 *Mammal Science*, 37, 2, 577-610

786 Russo, D, Sgammato, R., Bosso, L., 2016. First sighting of the humpback whale *Megaptera*
787 *novaeangliae* in the Tyrrhenian Sea and a mini-review of Mediterranean records. *Hystrix, the*
788 *Italian Journal of Mammalogy* 27(2), 219–221. doi: <https://doi.org/10.4404/hystrix-27.2-11737>

789 Schäfer, W., 1972. *Ecology and Palaeoecology of Marine Environments*. The University of Chicago
790 Press, Chicago, 568 pp.

791 Smith, C.R., Baco, A.R., Glover, A., 2002. Faunal succession on replicate deep-sea whale falls: time
792 scales and vent-seep affinities. *Cahiers de Marine Biologie* 43, 293–297.

793 Smith, C.R., Baco A.R., 2003. Ecology of whale falls are the deep-sea floor. *Oceanography and*
794 *Marine Biology: an Annual Review*, 41, 311–354. <https://doi.org/10.1201/9780203180570>

795 Smith, C.R., Bernardino, A.F., Baco, A.R., Hannides, A.K., Altamira, I., 2014. Seven-year
796 enrichment: macrofaunal succession in deep-sea sediments around a 30 tonne whalefall in the
797 Northeast Pacific. *Marine Ecology Progress Series* 515, 133–149. doi: 10.3354/meps10955

- 798 Smith, C.R., Glover, A.G., Treude, T., Higgs, N.D, Amon, D.J., 2015. Whale-Fall Ecosystems:
799 Recent Insights into Ecology, Paleoecology, and Evolution. *Annual Review of Marine Science* 7,
800 571–596.<https://doi.org/10.1146/annurev-marine-010213-135144>
- 801 Spano, C., 1989. Macrofauna circalitorale del Pliocene inferiore di Capo S. Marco (Sardegna
802 occidentale). *Rivista Italiana di Paleontologia e Stratigrafia* 95 (2), 137-172.
803 <https://doi.org/10.13130/2039-4942/10630>
- 804 Taylor, J.D., Glover, E.A., 2005. Cryptic diversity of chemosymbiotic bivalves: a systematic
805 revision of worldwide Anodontia (Mollusca: Bivalvia: Lucinidae). *Systematics and Biodiversity*
806 3 (3), 281–338.<https://doi.org/10.1017/S1477200005001672>
- 807 Taylor, J.D., Glover, E.A., 2006. Lucinidae (Bivalvia) - The most diverse group of chemosymbiotic
808 molluscs. *Zoological Journal of the Linnean Society* 148, 421–
809 438.<https://doi.org/10.1111/j.1096-3642.2006.00261.x>
- 810 Tirado, C., Rueda, J.L., Salas, C., 2011. Reproductive cycles in Atlantic and Mediterranean
811 populations of *Venus nux*Gmelin, 1791 (Bivalvia: Veneridae), from southern Spain. *Journal of*
812 *Shellfish Research* 30 (3), 813–820.<https://doi.org/10.2983/035.030.0322>
- 813 Tomlin, A. G. 1967. Mammals of the USSR and adjacent countries. Cetacea. Vol. IX. Translation
814 from Russian, Israel Program for Scientific Translation, Jerusalem. 717 pp.
- 815 Tropeano, M., Sabato, L., 2000. Response of Plio-Pleistocene mixed bioclastic-lithoclastic
816 temperate water carbonate systems to forced regressions: the Calcarene di Gravina Formation,
817 Puglia, SE Italy. *Geological Society, London, Special Publication* 172, 217-
818 243.<https://doi.org/10.1144/GSL.SP.2000.172.01.11>
- 819 Tropeano, M., Sabato, L., Pieri, P., 2002a. Filling and cannibalization of a foredeep: the Bradanic
820 Trough, southern Italy. *Geological Society, London, Special Publication* 191, 55-
821 79.<https://doi.org/10.1144/GSL.SP.2002.191.01.05>
- 822 Tropeano, M., Sabato, L., Pieri, P., 2002b. The Quaternary "post-turbidite" sedimentation in the
823 South Apennines foredeep (Bradanic Trough-Southern Italy). *Bollettino della Società Geologica*

824 Italiana, Volume Speciale 1, 449-454.

825 Tropeano, M., Sabato, L., Festa, V., Capolongo, D., Casciano, C.I., Chiarella, D., Gallicchio, S.,
826 Longhitano, S.G., Moretti, M., Petruzzelli, M., Schiuma, G., Spalluto, L., Boenzi, F., Pieri, P.,
827 2018. "Sassi", the old town of Matera (southern Italy): first aid for geotourists in the "European
828 Capital of Culture 2019". *Alpine and Mediterranean Quaternary* 31 (2), 133 -
829 145. <https://doi.org/10.26382/AMQ.2018.09>

830 Tsai, C.H., Collareta, A., Fitzgerald, E.M.G., Marx, F.G., Kohno, N., Bosselaers, M., Insacco, G.,
831 Reitano, A., Catanzariti, R., Oishi, M., Bianucci, G., 2017. Northern pygmy right whales
832 highlight Quaternary marine mammal interchange. *Current Biology* 27, R1037–
833 R1059. <https://doi.org/10.1016/j.cub.2017.08.056>

834 Tsai, C.H., Chang, C.H., 2019. A right whale (Mysticeti, Balaenidae) from the Pleistocene of
835 Taiwan. *Zoological Letters* 5, 37. <https://doi.org/10.1186/s40851-019-0153-z>

836 Van Beneden, P.J. and Gervais, P. 1868–1879. *Ostéographie des cétacés vivants et fossiles,*
837 *comprenant la description et l'iconographie du squelette et du système dentaire de ces animaux,*
838 *ainsi que des documents relatifs à leur histoire naturelle. Atlas, 64 plates. Paris: A. Bertrand ed.*
839

840 **FIGURE CAPTIONS**

841

842 **Figure 1.A**, Mediterranean map with the location of the main Pleistocene records of baleen whales
843 including the here described skeleton of *Balaenoptera* sp. (MST Q1) collected near Bari from the
844 Calcarenite di Gravina Formation. The main surface water circulation is also reported.

845 Abbreviations: AW = Atlantic Water; MAW = Modified Atlantic Water; AIS = Atlantic Ionian
846 Stream. **B**, schematic map of Early Pleistocene paleogeography of southern Italy (from Tropeano et
847 al., 2002, modified).

848

849 **Figure 2**. Skeleton of *Balaenoptera* sp. (MST Q1) from the Lower Pleistocene Calcarenite di
850 Gravina Formation. The fossil is partially embedded in hard matrix and exposed dorsal side-up. The
851 small circles indicate the position of the associated fossil fauna and fossil traces on the bones.

852 Abbreviations: b1 = *Anodontia cf. fragilis*; b2 = *Acanthocardia echinata*; b3 = *Gibbula magus*; b4 =
853 *Venus nux*; st = shark tooth; stb = shark tooth bite marks.

854

855 **Figure 3**. Skeleton of *Balaenoptera* sp. (MST Q1) from the Lower Pleistocene Calcarenite di
856 Gravina Formation. **A**, fragmentary cranium and mandibles; **B,C**, posterior portion of the skull,
857 cervicals, thoracics, ribs, and portion of the right forelimb regions. Note the shark tooth near the
858 distal end of the left fourth rib. Linear hatching indicates major breaks. For the colours associated
859 with the different bones, see figure 2.

860

861 **Figure 4**. Tympanic bullae associated to the skeleton of *Balaenoptera* sp. (MST Q1) from the
862 Lower Pleistocene Calcarenite di Gravina Formation. **A-D**, right tympanic bulla still partially
863 embedded in hard matrix in anterodorsal (A,B), dorsal (C), and lateral (D) views; **E,F**, left tympanic
864 bulla removed by the matrix in dorsal (E) and medial (F) views. Linear hatching indicates major
865 breaks.

866 **Figure 5. A,B,D-G**, skeleton of *Balaenoptera* sp. (MST Q1) from the Lower Pleistocene
867 Calcarenite di Gravina Formation: proximal portion of the double-headed first left rib (A,B);
868 incomplete right scapula and right humerus (D,E); and left radius and ulna (F,G). C, proximal
869 portion of the double-headed first left rib of *Balaenoptera borealis* (MSNUP M262). Linear
870 hatching indicates major breaks. For the colours associated with the different bones, see figure 2.
871

872 **Figure 6.** Comparison of the first double-headed rib of *Balaenoptera borealis* and *B. edeni*
873 (redrawn from Omura, 1959, pl. 6, fig. 1) with the first rib of a juvenile of *Caperea marginata*
874 (redrawn from Buchholtz, 2011, fig. 2D), and with the anomalous first ribs of *Balaenoptera*
875 *musculus* (redrawn from Dubar, 1828, pl. 8) and *Eschrichtius robustus* (redrawn from Slijiper, 1936,
876 fig. 131). Scale bars equal 10 cm.

877
878 **Figure 7.** Vertebral count and centrum length (CL) in *Balaenoptera* sp. (MST Q1) and the
879 following other balaenopterids: *Balaenoptera edeni* (WRI 77M62, measurements from Omura et al.
880 1981); *B. borealis* (MSNUP M262), *B. physalus* (MSNUP M251), *B. musculus* (MSNUP M250), *B.*
881 *acutorostrata* (MSNUP M260), and *Megaptera novaeangliae* (MSNUP M263).

882
883 **Figure 8.** Comparison of the shape in lateral view and ratios of main measurements of the humerus,
884 radius, and ulna of MSTQ1 with the balaenopterids *Incakujira anillodefuego* (redrawn from Marx
885 and Kohno, 2016, fig. 14), *Megaptera novaengliae*, *Balaenoptera edeni* (redrawn from Omura,
886 1959, pl. 5, fig. 3), *B. musculus*, *Balaenoptera borealis*, *B. physalus*, *B. acutorostrata*, and
887 ‘*Megaptera*’ *hubachi* (redrawn from Bisconti, 2010, fig. 15). Scale bars equal 10 cm.

888

889 **Figure 9.** Skeleton of *Balaenoptera* sp. (MST Q1) from the Lower Pleistocene Calcarenite di
890 Gravina Formation: close ups of the associated fossil fauna and fossil traces. A, articulated
891 specimen of *Venus nux* located between the epiphysis and the respective centrum of one of the first
892 lumbar (b4 in fig. 2); B, *Carcharodon carcharias* tooth located near the distal end of the fourth left
893 rib (st in fig. 2); C, shark bite marks on the seventh? right rib (stb in fig. 2).

894

895

896 **TABLE CAPTION**

897

898 **Table 1.** Measurements (in millimetres) of the skeleton of *Balaenoptera* sp. (MST Q1).

899

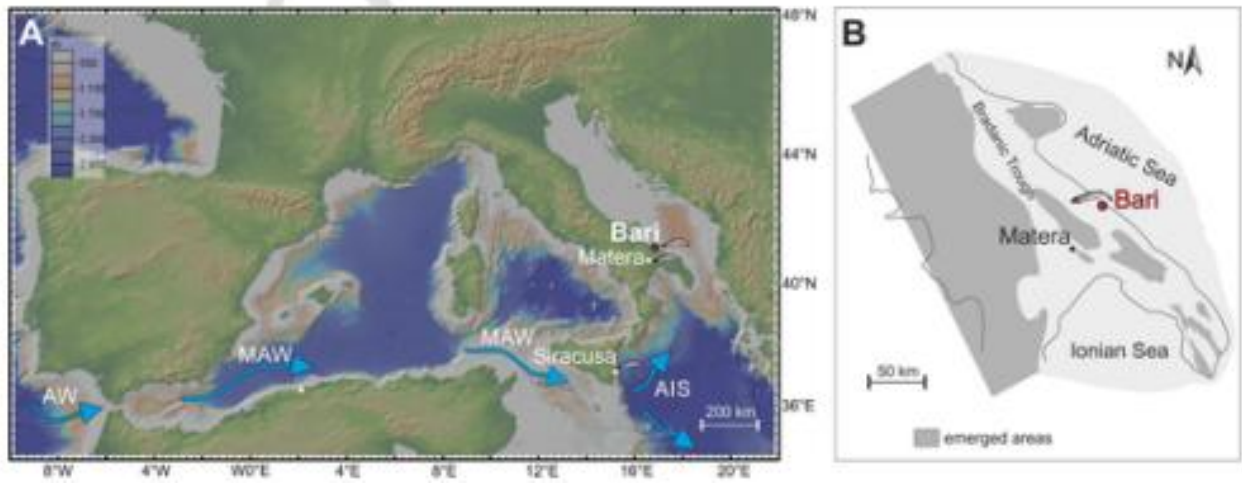


Fig 1



Fig. 2

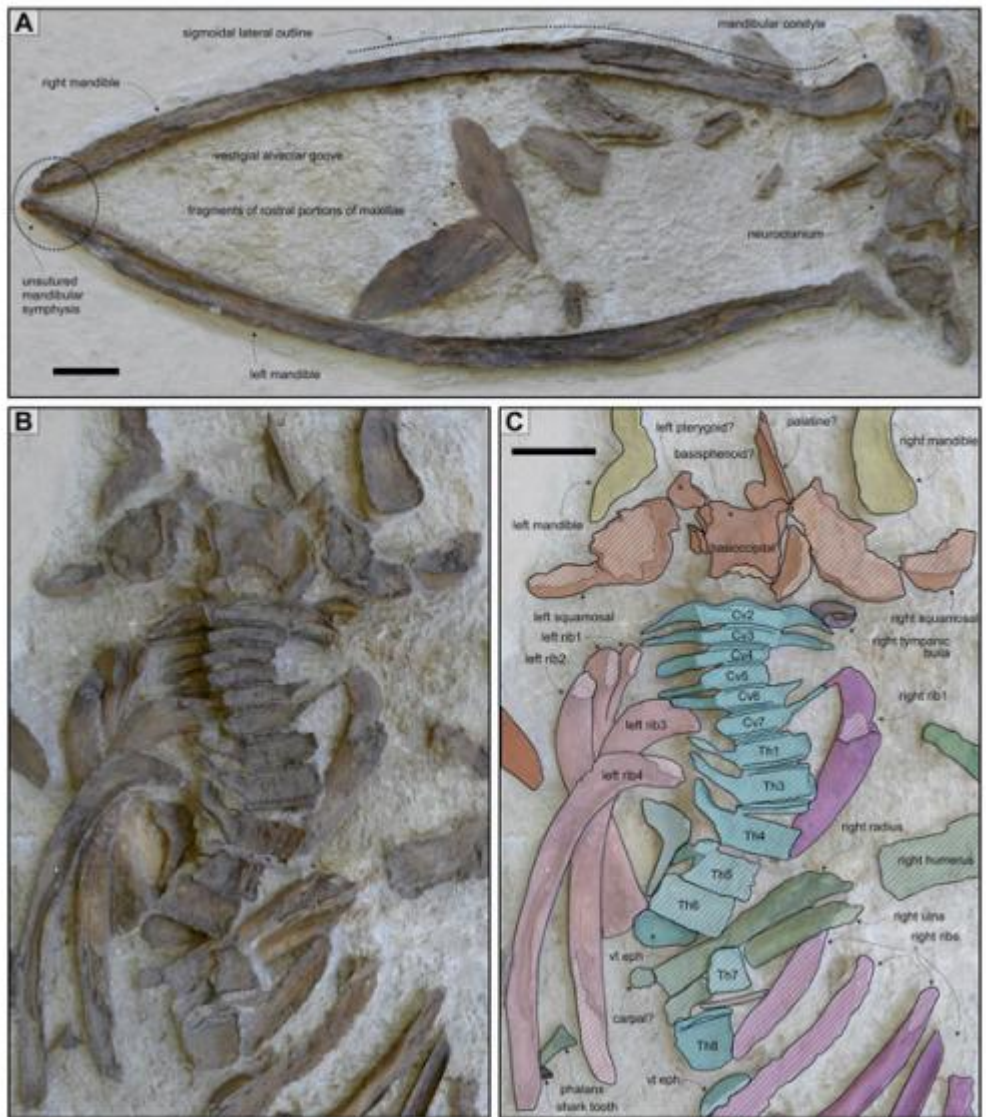


Fig 3

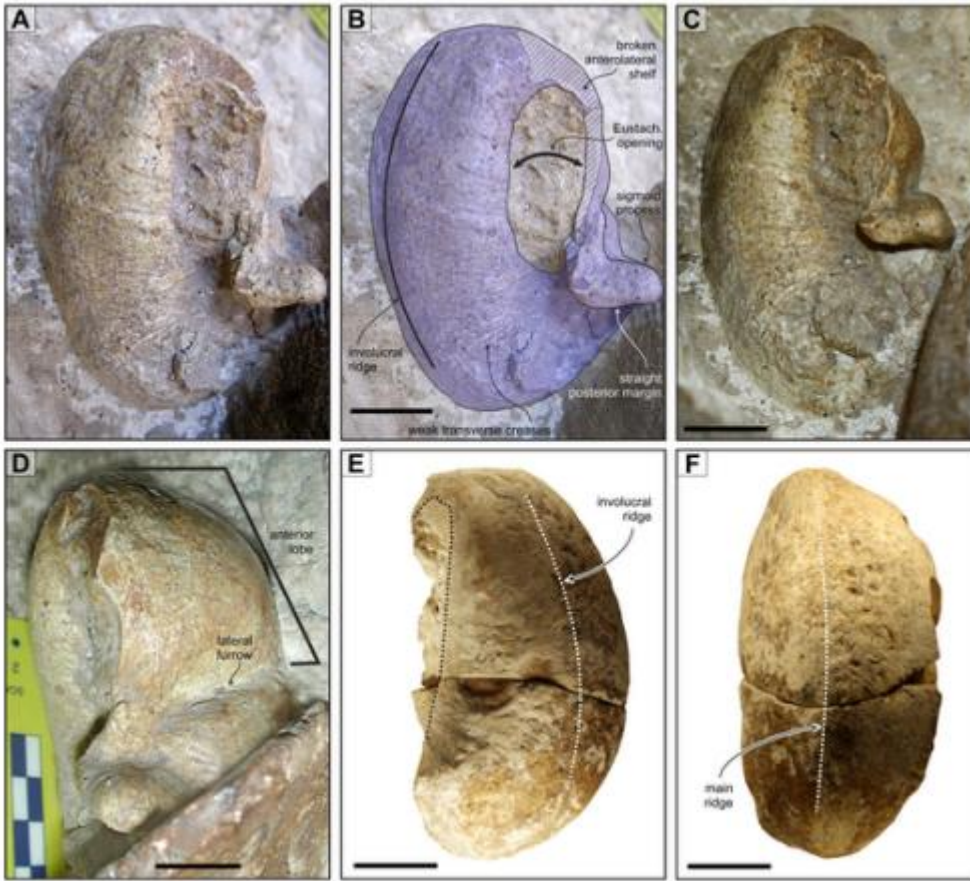


Fig 4

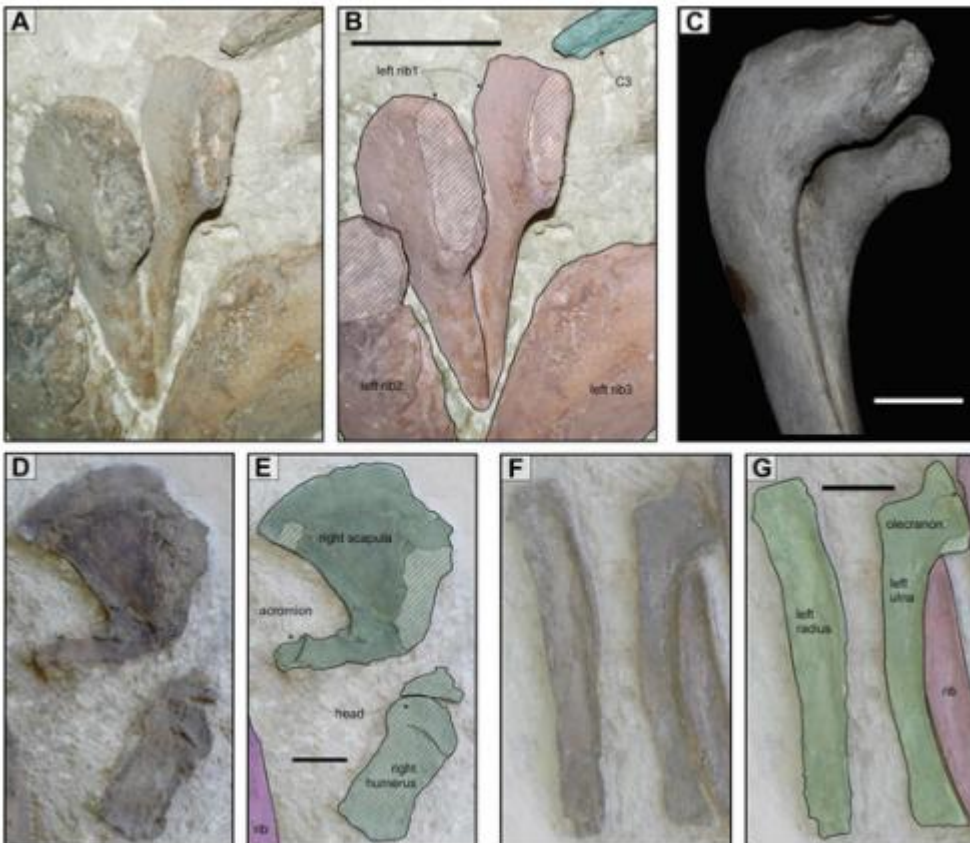


Fig 5

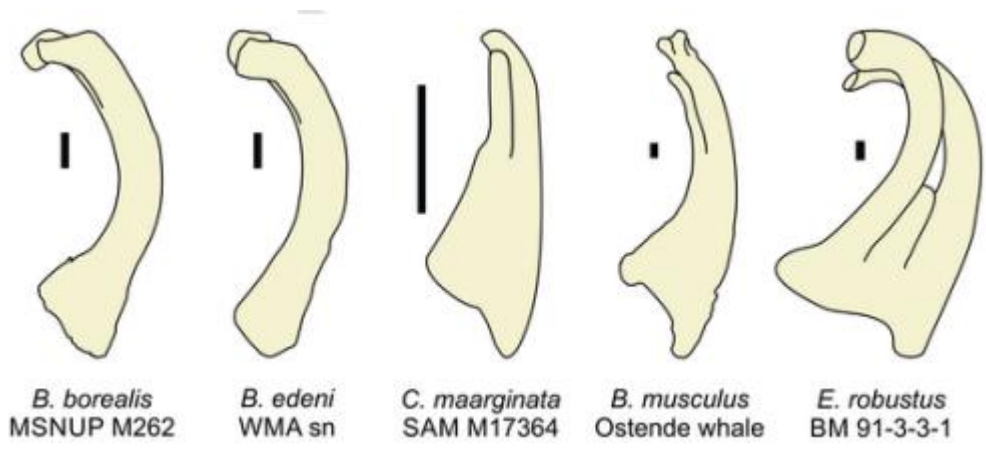


Fig 6

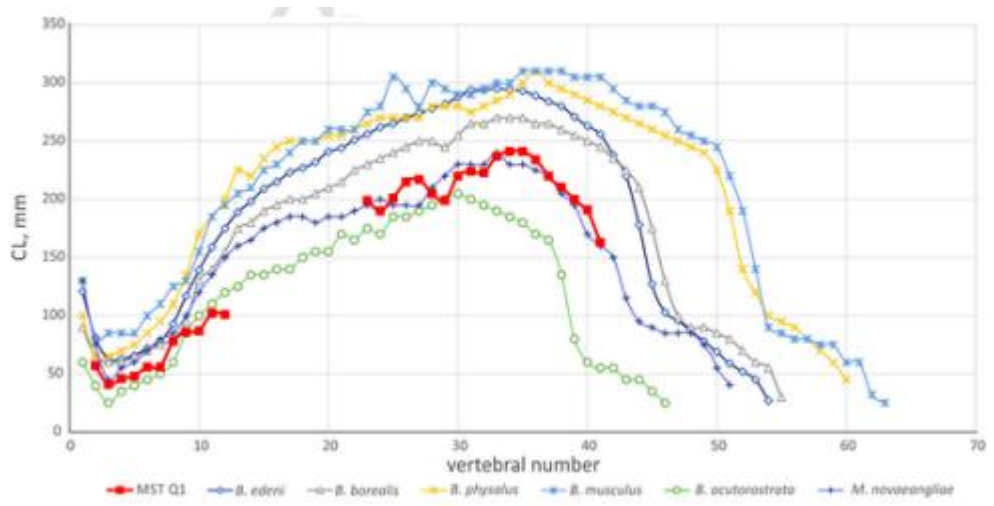


Fig 7

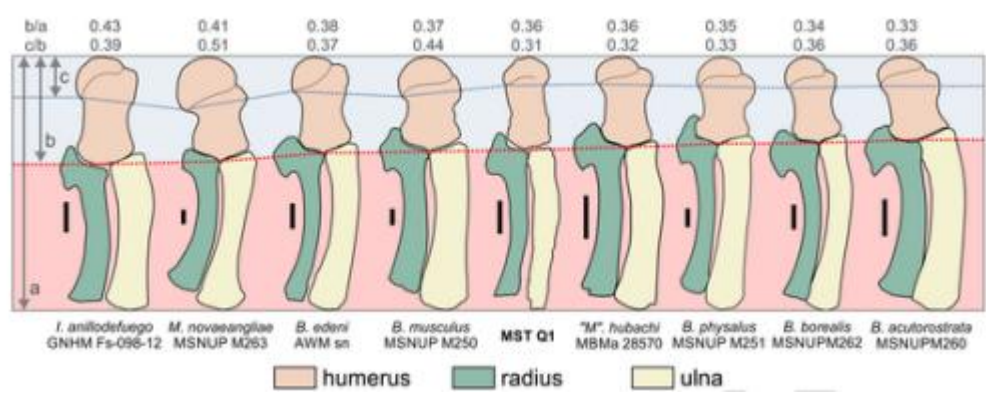


Fig 8

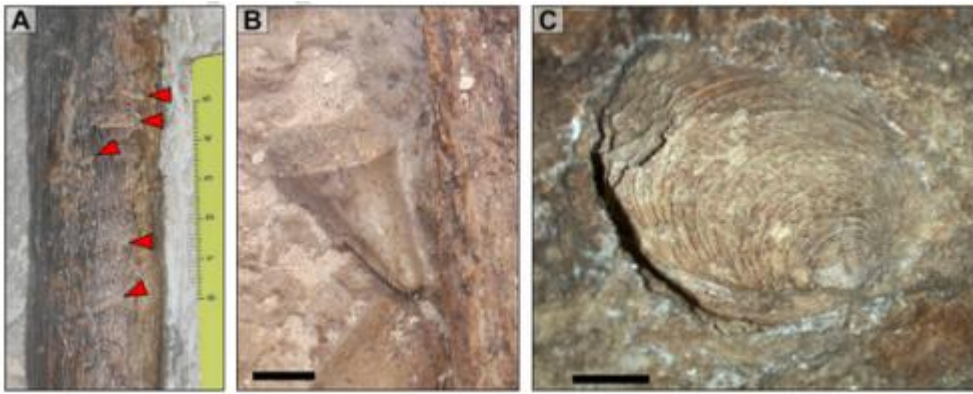


Fig 9